PERGAMON

Journal of Asian Earth Sciences 21 (2002) 7–21

Journal of Asian Earth Sciences

www.elsevier.com/locate/jseaes

Postcollisional granites in the South Tien Shan Variscan Collisional Belt, Kyrgyzstan

L.I. Solomovich[a,*], B.A. Trifonov[b]

[a]*Kyrgyz Mining and Metallurgical Institute, Bishkek, Kirgiziya*
[b]*Department of Geology, Sankt-Peterburg University, Russian Federation*

Received 15 December 2000; revised 16 November 2001; accepted 13 December 2001

Abstract

Two major types of the potassium-rich postcollisional granites of Permian age were studied in the South Tien Shan Variscan Collisional Belt. The first type, metaluminous granites of the Jangart complex, are located along the southeastern boundary of this belt with the Precambrian Tarim Block. The plagioclase rims on K-feldspar megacrysts (rapakivi texture), extremely high $FeO^t/(FeO^t + MgO)$ ratio, indications of the low H_2O and O_2 fugacities, high concentrations of the incompatible elements especially light rare earth elements (LREE), Ba, Nb along with heightened contents of the compatible elements especially Ni, Cr and moderately initial $^{87}Sr/^{86}Sr$ ratio ($Sr_0 = 0.7075$) make those granites similar to other rapakivi granites. The second type, peraluminous granites of the Inylchek complex, is located along the northwestern boundary of the belt with the Caledonian Kazakh Microcontinent. Those granites are rich in F, B, Li, Rb, Cs, Sn, Ta and heavy rare earth elements (HREE), but are poor in Ba, Sr, Ni and Cr and are characterized by the relatively high initial $^{87}Sr/^{86}Sr$ ratio ($Sr_0 = 0.7098$). Li–mica granites are distributed widely among them. The granites of a transitional type (Uchkoshkon complex) occupy an intermediate geographic position between major granite types. The initial Sr isotopic composition of the transitional granites varies widely (Sr_0 from 0.7080 to 0.7256). The variation in chemical composition of the coeval postcollisional granites across the Collisional belt, together with the variability of initial Sr isotopic ratios of the transitional granites, are thought to indicate basement heterogeneity. This heterogeneity, in turn, is probably related to thrusting of the Tarim Block under South Tien Shan during the collision.

Keywords: Postcollisional granites; South Tien Shan Variscan Collisional Belt; Kyrgzstan

1. Introduction

The Late Paleozoic thrust and fold structures of the South Tien Shan Collisional belt are part of the Ural—South Tien Shan linear Collisional system, formed during the closing of the Turkestan branch of the Paleoasian Ocean (Zonenshine et al., 1990). The Precambrian Tarim block was overridden by the Caledonian Kazakh microcontinent along the Southern Tien Shan part of that Collisional system to the east of the Talas-Fergana strike–slip fault (Byske, 1996). The syncollisional igneous rocks of Carboniferous age occur widely in the Karakum and Turkestan-Alai segments of the South Tien Shan folded belt to the west of the Talas-Fergana strike–slip fault. They are represented by various granitoids (mainly by granodiorites) of the calc–alkalic petrochemical series (Hamrabaev and Simon, 1984). To the east of the Talas-Fergana strike–slip fault, in the Kokshal segment of the South Tien Shan folded belt, the syncollisional granitoids are relatively rare and occur exclusively in the zone of the Atbashi-Inylchek marginal fault, which separates the collision belt from the Kazakh microcontinent. Another feature of the Kokshal segment is the abundance of potassium-rich subalkaline postcollisional granites and leucogranites of Permian age (Byske et al., 1996; Solomovich and Malukova, 2000). In the study area, located in the eastern part of the Kokshal segment, postcollisional granites are widely distributed and represented by various geochemical types. It is very likely that the variability in petrographical, geochemical and Sr isotopic compositions of the postcollisional granites across the Collisional belt strike zone is a consequence of continental crustal heterogeneity above the continental subduction zone. The purpose of this study is to present petrological, geochemical, and Sr isotopic data on the postcollisional granites in order to determine the character of the continental crust

* Corresponding author. Present address: Technocon International, Inc., 1111 Kane Concourse, Suite 518 Bay Harbor Islands, Florida 33154, USA. Tel.: +1-305-867-1228; fax: +1-305-867-1637.
E-mail address: solomovich@the-beach.net (L.I. Solomovich).

1367-9120/02/$ - see front matter
PII: S1367-9120(02)00008-1

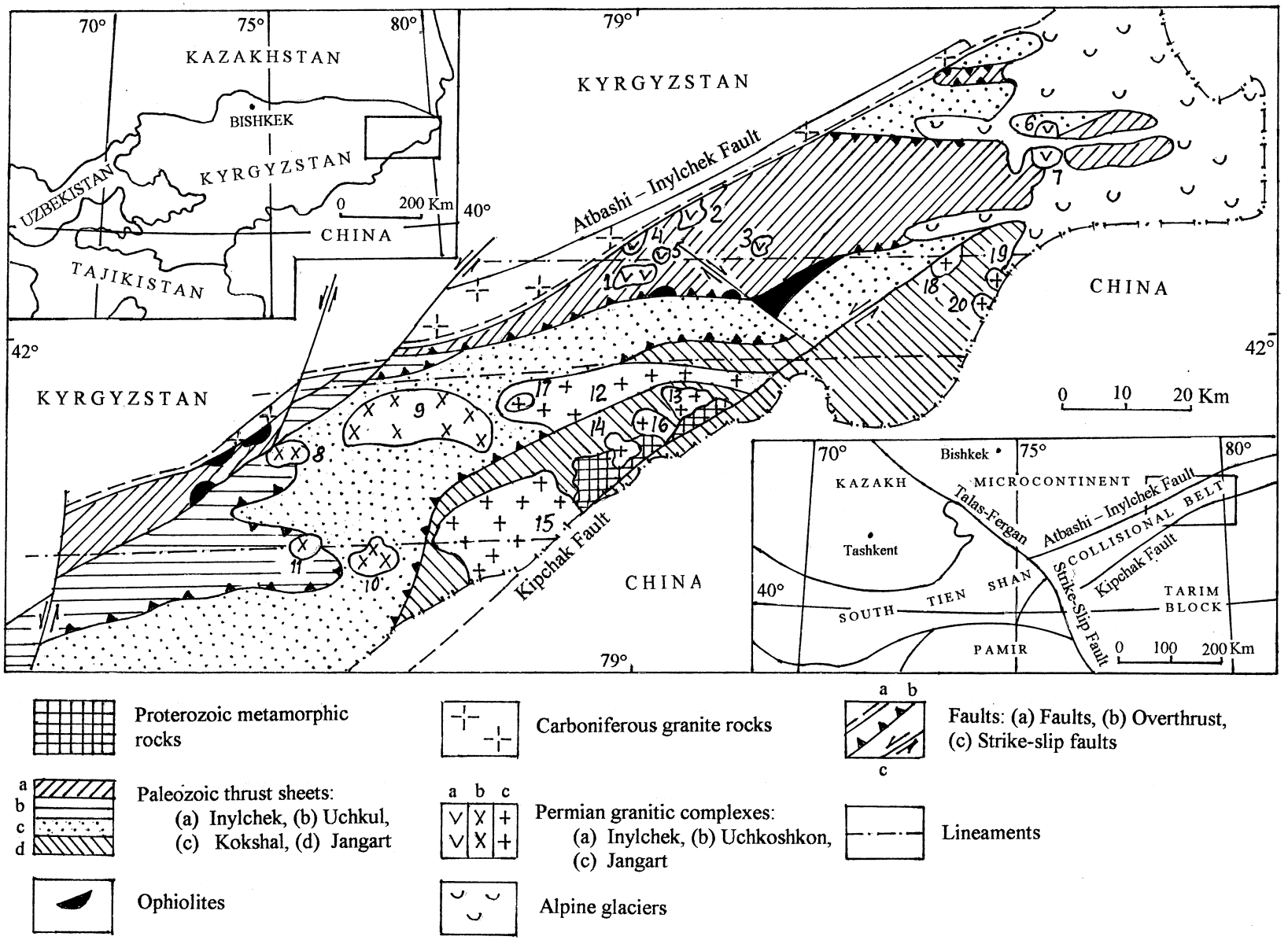

Fig. 1. General geology of the Saryjaz section of the South Tien Shan Variscan Collisional Belt. Names of the Permian granite intrusions. Inylchek complex: 1—Tashkoro, 2—Maidadir, 3—Atjailau, 4—Inylchek, 5—Suchodol, 6—North Komsomol, 7—South Komsomol; Uchkoshkon complex: 8—Aktash, 9—Uchkoshkon, 10—Pikertyk, 11—Sarybulak; Jangart complex: 12—Akshiurak, 13—Karagaity, 14—Sauktor, 15—Jangart, 16—Jetikait, 17—Akchiy, 18—Maybash, 19—Iransu, 20—Ara.

into which they were emplaced. Furthermore, the postcollisional granites are of economic interest, since they contain Sn–W deposits of the Saryjaz ore-bearing area that are economically important for the Kyrgyz Republic and the whole Central Asian region.

2. Geologic background

The study area, known as the Saryjaz syntaxis (Khristov, 1989), is the narrowest part of the South Tien Shan Variscan Collisional Belt and lies between the Caledonian Kazakh microcontinent to the north-west and the Precambrian Tarim block to the south-east (Fig. 1). The Saryjaz syntaxis is made up of a series of folded overthrusts, which were thrust southward during the Carboniferous period (Porshniyakov, 1983; Byske et al., 1985). The Late Paleozoic ophiolitic melanges occur along the Atbashy-Inylchek fault, which separates the collision belt from the Kazakh microcontinent. These ophiolitic melanges are believed to be produced by the collision between a passive continental margin on the north side of the Tarim block and an active continental margin on the south side of the Kazakh microcontinent (Bakirov et al., 1989; Byske, 1996; Gao et al., 1997). The ophiolite assemblage is deformed by the sinistral strike–slip displacements (Khristov, 1989). A similar sense of motion is also observed along the Kipchak fault, which separates the Collisional belt from the Tarim block (Fig. 1). The sublatitudinal sinistral strike–slip displacements of Permian age are common in the Tien Shan and the adjoining territories (Allen et al., 1995). According to Bazhenov et al. (1999), the Permian sinistral shear zone, which is about 300 km wide, is traced along Tien Shan fold belt for 2500 km. In the Saryjaz syntaxis, the sinistral displacements are considered a consequence of oblique continental subduction of the Tarim block under the Kazakh microcontinent (Byske, 1996). The oblique collision between the above-mentioned microcontinents with subsequent A-type subduction of the Tarim continental crust and lithosphere-scale sinistral shearing are corroborated by the paleomagnetic data (Chen et al., 1997; Bazhenov et al., 1999).

Two processes caused the principal peculiarities of the geological structure of the study area: the syncollisional crustal thickening and postcollisional vertical block movements (Trifonov and Solomovich, 1993). The pile of folded overthrusts, consisting of no less then eight overthrust sheets (Byske, 1996), was formed during the Middle and Late Carboniferous as a result of the syncollisional crustal thickening. The thrust sheets are divided into four packages that are exposed in a succession—the lowest package is in the south and the uppermost one is in the north (Fig. 1).

The Jangart package is the lowest of these thrust sheets. It consists of the carbonate-rich formations, which formed on the continental shelf of the Tarim microcontinent northern passive margin. The structural thickness of the package is about 2000 m and the age is Silurian to Carboniferous (Byske et al., 1985).

The Kokshal package lies to the north, structurally above the Jangart. It consists of flysch formations that accumulated on the continental slope of the Tarim microcontinent. The structural thickness of the package is about 5000 m and the age is also Silurian to Carboniferous (Byske et al., 1985).

The Inylchek (10,000 m) and Uchkul (4500 m) packages crown the succession of thrust sheets. They are exposed in the northern part of the belt and include overthrust sheets that consist of heterogeneous volcanic and sedimentary formations of the southern active margin of the Kazakh microcontinent. Both of packages are of Devonian to Carboniferous in age (Byske et al., 1985).

The overthrust sheets together represent the upper 15–20 km of continental crust, which is about 65 km thick in this area (Knauf, 1986).

There are two periods of granitic magmatism preserved in the Saryjaz syntaxis (Trifonov and Solomovich, 1993). The first is syncollisional calc–alkalic granitic plutonism of Middle to Late Carboniferous age. This plutonism is represented by the abyssal batholith of Terekty, which is emplaced along the Atbashy-Inylchek marginal fault (Fig. 1) and is not considered in this study. The second period of granite magmatism occurred during the Permian. These postcollisional hypabyssal granites, which are the subject of this study, can be subdivided into three different groups on the basis of petrology, geochemistry and Sr isotopic composition.

3. Sampling and analytical methods

Fifteen granitic bodies were sampled in the Saryjaz segment of the South Tien Shan. The samples were taken from principal rock facies and their varieties. After examination of the thin sections, samples with indications of epigenetic hydrothermal alterations were rejected. Unaltered samples were trimmed of weathered material and about 2–5 kg of rock were crushed for analysis.

Geochemical and isotopic analyses for this study were carried out at the Irkutsk Geochemistry Institute of the Siberian Branch of the Russian Science Academy. Major elements were determined by the wavelength-dispersion X-ray fluorescence spectrometry (XRF). Analysis for Li, Rb, Cs were performed by the flame-photometric method. The concentration of fluorine was determined by chemical analysis. The rest of the trace elements, including REE, were analyzed by ICP emission spectrophotometry using natural rock standards as reference samples for calibration. Isotopic analyses were done on a MI 1201 'T' mass spectrometer. The concentrations of Sr and Rb were determined by the isotope dilution method. Relative errors of analyses were 0.015–0.3% for $^{87}Sr/^{86}Sr$ and 0.1–0.8% for $^{87}Rb/^{86}Sr$. The average $^{87}Sr/^{86}Sr$ value of VNIIM-Sr

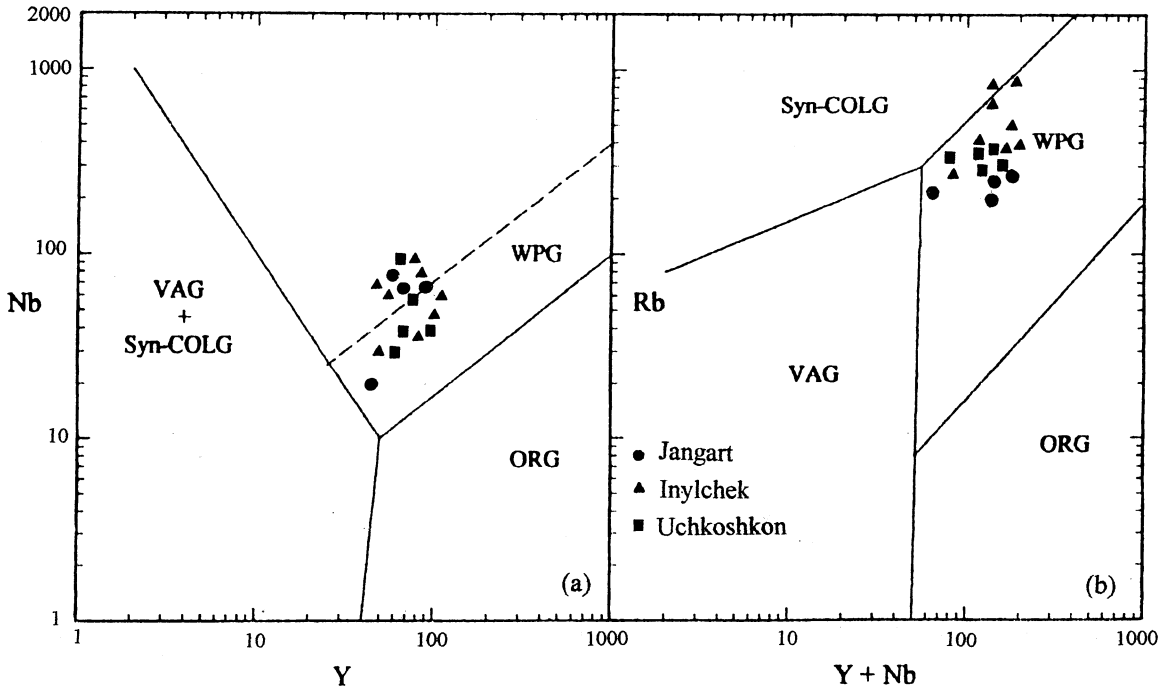

Fig. 2. (a) Nb vs Y and (b) Rb vs Y + Nb discrimination diagrams for postcollisional granites from South Tien Shan showing the tectonic classification suggested by Pearce et al. (1984). ORG, ocean ridge granite; Syn-COLG, syn-collision granite; VAG, volcanic arc granite; WPG, within plate granite.

standard obtained during the measuring campaign was 0.70810 ± 10.

4. Description of postcollisional granites

Postcollisional granites were emplaced after the formation and consolidation of the thrust and fold structure of the South Tien Shan Collisional belt in the region of vertical block movements (Trifonov and Solomovich, 1993). According to Bazhenov et al. (1999), an area of Permian magmatism in the North and South Tien Shan is interpreted as an extensional domain conjugated with the above mentioned shear zone. The postcollisional granitic bodies are discordant with Paleozoic country rocks (Trifonov and Solomovich, 1993) and form E–W-striking chains (Fig. 1) which intersect the fold structure obliquely. Such an arrangement of these granites contrasts with the elongation of the syncollisional granites along the marginal Atbashy-Inylchek fault concordantly with the strike of the Collisional belt. The postcollisional emplacement of the granites under consideration is corroborated by the location of the rock chemical compositions in the field of within plate granite based on Nb vs Y and Rb vs Y + Nb discriminate diagrams (Fig. 2).

Postcollisional granites of the Saryjaz syntaxis occur in different thrust sheet packages and can be subdivided into three igneous complexes: Jangart, Inylchek, and Uchkoshkon.

4.1. Jangart complex

Intrusions of the Jangart igneous complex are exposed along the boundary of the Variscian Collisional belt and the Tarim block. They occur in the lowest Jangart thrust package. The complex includes two large plutons, the Akshiyrak (about 450 km^2) and the Jangart (about 350 km^2), as well as the small satellites: Sauktor, Karagaity, Jetikait, Maybash, Iransu and Ara intrusions (Fig. 1). The granites cut through and metamorphose fossil-bearing sediments varying in age from Silurian to the Upper Carboniferous. The contacts with the country rocks are sharp and often obscured by later faulting. Biotite and feldspar–pyroxene–amphibole hornfels and marbles developed in zones of exometamorphism, which have a width of about 100–150 m. In zones of endometamorphism, granites grade into granite–porphyries with cryptic (nevaditic) texture. The near-roof and near-base zones of endometamorphism contain xenoliths of melanocratic rocks, ranging in size from tens of centimeters up to 200 m. The compositions of these xenoliths vary from monzodiorite to melanosyenite.

The Jangart complex was formed by successive emplacement of three intrusive phases (Solomovich and Trifonov, 1990): (1) coarse-grained rapakivi granite and rapakivi quartz syenite; (2) medium-grained hastingsite–biotite granites; (3) fine-grained hastingsite–biotite leucogranites. Both the Jangart and Akshiyrak plutons consist mainly of rapakivi granite and rapakivi quartz syenite which grade into one other, although rapakivi granite is more common in the Akshiyrak pluton whereas the Jangart pluton is dominated by quartz syenite. In both plutons, the rocks are

Table 1
Major (wt%) and trace (ppm) element concentration of granitic rocks from South Tien Shan (^{t}total iron as Fe_2O_3; A/CNK is molar $Al_2O_3/(CaO + Na_2O + K_2O)$; NK/A is molar $(Na_2O + K_2O)/Al_2O_3$; F/FM is molar $Fe_2O_3^t/(Fe_2O_3^t + MgO)$; Grsy-rpk: granosyenite rapakivi; Gr-rpk: granite rapakivi; Has-gr: hastingsite-biotite granite; Has-lcgr: hastingsite-biotite leucogranite; Q-monz: quartz monzonite; Bi-gr: biotite granite; Bi-lcgr: biotite leucogranite; Li-lcgr: Li-mica leucogranite)

Complex	Jangart														
Pluton	Jangart			Akshiyrak					Sauktor	Akchiy		Jetikait	Maybash	Iransu	
Sample	TF251	D26	D35	A11	A75	A29	TF91	A16	A102	A204	A208	SH68	SH500	SH12	SH302
Description	Grsy-rpk	Grsy-rpk	Gr-rpk	Gr-rpk	Gr-rpk	Gr-rpk	Gr-rpk	Gr-rpk	Gr-rpk	Has-gr	Has-gr	Has-gr	Has-gr	Has-lcgr	Has-lcgr
SiO_2	65.06	64.92	67.1	67.6	68.05	68.2	68.25	69.7	71.54	71.96	72.64	71.76	70.65	73.89	75.97
TiO_2	0.55	0.49	0.58	0.63	0.53	0.49	0.44	0.52	0.32	0.26	0.26	0.18	0.27	0.15	0.13
Al_2O_3	14.48	16.3	15.12	14.44	13.9	14.05	13.36	13.58	13.56	12.95	13.04	12.96	13.42	11.85	10.93
$Fe_2O_3^t$	6.26	5.2	5.21	4.95	4.48	4.76	5.53	4.01	3.32	2.55	2.81	3.14	4.23	2.9	2.63
MnO	0.11	0.08	0.07	0.05	0.06	0.06	0.09	0.05	0.04	0.03	0.03	0.07	0.08	0.04	0.03
MgO	0.56	0.45	0.5	0.2	0.15	0.13	0.42	0.22	0.39	0.21	0.15	0.23	0.22	0.18	0.16
CaO	3.1	2.48	2.1	2.3	2.01	2.08	2.12	1.98	1.9	1.5	1.34	0.97	1.2	1.26	1.07
Na_2O	3.68	4.25	3.78	3.66	3.44	3.43	3.1	3.55	3.6	3.8	3.37	4.55	3.98	3.62	3.38
K_2O	5.4	5.1	5.36	5.11	5.5	5.39	5.35	5.4	4.39	5.01	4.86	5.02	5.13	4.91	4.44
P_2O_5	0.11	0.09	0.11	0.15	0.25	0.21	0.09	0.25	0.04	0.08	0.02	0.04	0.06	0.04	0.02
L.O.I.	0.29	0.4	0.35	0.24	0.9	0.5	0.48	0.55	0.32	0.87	0.78	0.46	0.18	0.39	0.32
Total	99.6	99.76	100.28	99.33	99.25	99.3	99.23	99.81	99.42	99.22	99.3	99.38	99.42	99.23	99.08
A/CNK	0.82	0.95	0.95	0.91	0.91	0.91	0.9	0.89	0.95	0.89	0.95	0.97	0.92	0.88	0.82
NK/A	0.82	0.77	0.8	0.81	0.83	0.82	0.82	0.86	0.8	0.9	0.87	1.01	0.91	0.94	1.03
F/FM	0.92	0.87	0.85	0.92	0.94	0.93	0.93	0.91	0.89	0.88	0.95	0.93	0.95	0.89	0.94
Li	24	28	45	25	39	32	36	49	46	35	59	65	33	24	10.3
Rb	223	220	269	190	215	203	268	216	155	230	256	341	284	265	227
Cs															
Sr	165	169	150	185	182	179	170	165	127	106	65	49	82	59	67
Ba	1425	1190	1235	1355	1400	1480	1250	1280	842	895	543	292	386	338	327
Sn	11	10	14	9.5	21	8.2	16	15	5.1	6.9	7.5	7.7	12.8	5.4	7.9
Pb	60	49	40	31	29	36	39	40	25	21	18	24	37	34	40
Zn	78	102	71	54	63	69	56	61	34	52	49	53	69	57	32
Ni	41	26	30	35	29	21	29	20	19	17	15	16	19	14.5	12.3
Co	12	7	6	11	9	8	7	5	4	5.5	6	4	5.3	2.5	3.8
Cr	41	39	35	64	75	59	82	51	38	34	29	27	29	25	17
Nb	68						78						71		20
Ta	7						13						5.7		1.1
Zr	335						470						710		228
Hf	4.6						6.5						14.2		6.4
Y	67						62						90		44
Be	2.2	3.1	2	2.6	2.8	3	3.6	3.8	3	2.5	4.5	3.1	5.1	2	2.4
B	34	18	21	14	26	23	47	19	5.5	12	43	66	19	8	5.7
F (wt%)	0.35	0.28	0.3	0.24	0.29	0.21	0.19	0.16	0.12	0.26	0.2	0.31	0.42	0.11	0.09
K/Rb	216	192	165	223	212	220	166	207	235	181	157	122	150	154	162
Ba/Rb	6.4	5.4	4.6	7.1	6.5	7.3	4.7	5.9	5.4	3.9	2.1	0.86	1.4	1.3	1.4
Nb/Ta	9.7						6						12.5		18.2
Zr/Hf	72.8						72.3						52.1		35.6

Table 1 (*continued*)

Complex	Uchkoshkon												Inylchek			
Pluton	Aktash	Uchkoshkon						Pikertyk			Sarybulak		Tashkoro			
Sample	U39	U124	U53	U17	U58	U81	U55	P16	P09	P42	S14	S11	T76/3	T115	T67	T61
Description	Q-monz	Bi-lcgr	Bi-lcgr	Bi-lcgr	Bi-lcgr	Bi-lcgr	Bi-lcgr	Bi-lcgr	Bi-lcgr	Bi-lcgr	Bi-lcgr	Bi-lcgr	Bi-gr	Bi-gr	Bi-gr	Bi-gr
SiO_2	64.7	72.58	72.9	73.06	73.48	73.71	74.21	73.38	73.82	74.5	73.7	73.95	70.21	70.99	71.45	72.19
TiO_2	0.45	0.28	0.26	0.3	0.2	0.19	0.15	0.3	0.18	0.12	0.32	0.21	0.35	0.34	0.22	0.27
Al_2O_3	16.2	13	13.26	12.99	13.12	12.83	12.6	12.35	12.45	12.88	12.6	13.2	13.8	13.95	13.9	14.1
$Fe_2O_3^t$	4.31	2.44	2.32	2.7	2.43	2.15	2.08	3.12	2.54	1.98	2.55	2.4	3.45	3.25	2.27	1.85
MnO	0.08	0.05	0.04	0.06	0.02	0.04	0.03	0.03	0.03	0.05	0.03	0.04	0.04	0.04	0.03	0.03
MgO	1.8	0.2	0.25	0.2	0.18	0.21	0.18	0.25	0.22	0.14	0.18	0.23	0.35	0.21	0.12	0.44
CaO	3.65	1.25	1.23	1.38	1.15	1.1	0.92	1.1	1.11	0.97	1.09	1.3	1.6	1.7	1.5	1.25
Na_2O	3.02	3.56	3.5	2.99	3.65	3.36	3.35	2.8	3.5	3.42	2.8	2.75	3.07	3.05	2.99	3.16
K_2O	4.94	5.02	4.99	5.77	5.31	5.29	4.85	5.69	4.72	4.89	5.58	5.64	5.15	5.41	5.48	5.66
P_2O_5	0.22	0.05	0.05	0.08	0.05	0.04	0.02	0.03	0.03	0.03	0.04	0.02	0.11	0.96	0.16	0.14
L.O.I.	0.32	0.75	0.32	0.76	0.54	0.46	0.8	0.57	1.5	0.64	0.53	0.46	1.04	0.53	1.3	0.8
Total	99.69	99.18	99.12	100.27	100.13	99.38	99.19	99.62	100.1	99.61	99.42	100.2	99.81	99.53	99.42	99.89
A/CNK	0.96	0.96	0.99	0.95	0.94	0.96	1.02	0.97	0.98	1.01	1	1.01	1.03	1.04	1.02	1.04
NK/A	0.63	0.87	0.84	0.86	0.89	0.88	0.85	0.87	0.86	0.85	0.84	0.81	0.75	0.76	0.78	0.8
F/FM	0.57	0.86	0.82	0.87	0.86	0.85	0.84	0.87	0.87	0.87	0.86	0.83	0.86	0.9	0.91	0.7
Li	39	132	164	110	105	129	192	63	84	76	58	62	121	105	148	132
Rb	225	365	392	340	326	312	434	232	294	310	225	280	384	346	360	370
Cs		18	26	16	14	21							18	14	21	16
Sr	375	108	91	89	71	75	84	69	65	79	73	54	179	168	175	105
Ba	930	450	480	345	390	375	285	365	420	360	590	475	555	610	480	430
Sn	6.4	15.4	17.5	19	14	21	32	10.9	14.3	16.3	8.9	11	30	18	21	26
Pb	18	45	39	51	42	38	48	36	39	31	33	44	36	41	32	50
Zn	58	72	58	61	49	55	60	147	79	68	115	86	55	62	49	81
Ni		7.9	6	6.6	4.9	4.3	5.2	10.2	7.2	6.5	8.3	6.8	12	6.8	5.2	4.3
Co		2.2	2.6	1.8	2.4	1.7	1.4	1.6	2.4	2	1.6	1.8	3	2.9	3.8	3.6
Cr		19	18	14	15	11	16	12	11	10	17	13	12	16	18	11
Nb		42		38		33			94			59	40		52	
Ta		3.9		2.9		2.8							4.8		6.1	
Zr		208		196		292			175			295	230		249	
Hf		6.6		6.9		9.5							6.9		7.9	
Y		89		69		50			66			83	76		99	
Be	1.6	5.2	6	5.9	7.5	5.5	7.1	4.8	6.2	4.1	5.3	3.9	8.1	7.4	6.3	9
B		17.5	20	28	26	19.5	37.5	78	132	95	15.5	22.5	34	39	45	29
F (wt%)	0.08	0.25	0.29	0.28	0.2	0.16	0.18	0.22	0.19	0.25	0.13	0.12	0.23	0.19	0.15	0.29
K/Rb	182	114	106	140	135	141	93	161	133	131	157	167	112	130	126	127
Ba/Rb	4.1	1.2	1.2	1	0.98	1.2	0.66	1.25	1.4	1.2	2	1.7	1.4	1.8	1.3	1.2
Nb/Ta		10.8		13.1		11.8							8.3		8.5	
Zr/Hf		31.6		28.1		30.5							33.2		31.5	

Table 1 (*continued*)

Complex																	
Pluton	Maidadir			Komsomol				Inylchek			Komsomol			Suhodol			
Sample	M17	M22	M13	K101	K93	K32	K106	I22	I09	I16	K115	K130	K1000	S46	T99/8	T90/1	T96/7
Description	Bi-gr	Bi-gr	Bi-gr	Q-monz	Bi-lcgr	Bi-lcgr	Bi-lcgr	Bi-lcgr	Bi-lcgr	Bi-lcgr	Li-lcgr	Li-lcgr	Li-lcgr	Li-lcgr	Li-lcgr	Li-lcgr	Li-lcgr
SiO_2	70.26	71.75	72.03	68.08	73.22	74.15	74.25	74.26	74.42	75.1	73.36	74.3	75.08	73.05	74.15	74.26	75.2
TiO_2	0.4	0.31	0.3	0.42	0.2	0.16	0.1	0.09	0.08	0.08	0.09	0.08	0.07	0.05	0.07	0.08	0.05
Al_2O_3	14.42	14.18	13.75	15.65	13.68	13.3	13.25	13.59	14.8	13.1	14.02	13.39	13.2	14.82	13.81	13.56	13.46
$Fe_2O_3^t$	2.59	2.49	2.55	3.64	2.45	1.9	1.96	0.87	0.6	0.8	2.04	2.03	1.91	1.2	1.51	1.8	1.2
MnO	0.04	0.04	0.04	0.05	0.03	0.05	0.03	0.03	0.03	0.03	0.06	0.04	0.04	0.03	0.04	0.04	0.02
MgO	0.62	0.33	0.35	1.13	0.18	0.09	0.08	0.09	0.1	0.12	0.09	0.12	0.27	0.08	0.1	0.12	0.1
CaO	1.75	1.39	1.23	2.92	1.01	0.66	0.78	0.68	0.71	0.81	0.67	0.7	0.92	0.72	0.7	0.69	0.53
Na_2O	3.19	3.66	3.59	3.09	3.19	4.06	3.63	3.05	4.05	3.82	3.65	3.77	3.56	5.5	3.93	3.88	3.89
K_2O	5.09	4.95	4.76	4.06	5.12	4.73	4.92	5.94	4.9	4.85	4.87	4.55	4.53	3.75	4.85	4.7	4.39
P_2O_5	0.15	0.16	0.12	0.07	0.04	0.03	0.02	0.03	0.02	0.02	0.02	0.03	0.02	0.02	0.02	0.02	0.02
L.O.I.	0.85	0.66	0.88	0.63	0.56	0.6	0.65	0.8	0.54	0.72	0.64	0.7	0.57	0.59	0.83	0.7	0.6
Total	99.36	99.92	99.6	99.74	99.68	99.73	99.67	99.43	100.25	99.45	99.51	99.71	100.21	99.81	100.01	99.85	99.46
A/CNK	1.03	1.02	1.04	1.06	1.1	1.03	1.05	1.07	1.11	1.02	1.11	1.08	1.06	1.04	1.06	1.07	1.12
NK/A	0.75	0.8	0.81	0.6	0.78	0.88	0.85	0.84	0.81	0.87	0.8	0.82	0.82	0.88	0.84	0.84	0.82
F/FM	0.7	0.81	0.8	0.65	0.87	0.9	0.9	0.79	0.73	0.77	0.9	0.9	0.79	0.85	0.87	0.86	0.85
Li	70	83	96	63	190	210	175	220	241	290	675	794	580	510	462	630	405
Rb	290	314	320	209	395	364	433	480	440	530	1100	1325	890	955	745	1005	836
Cs				10	35	28	33	39	42	65	122	144	93	116	70	84	105
Sr	163	131	85	345	92	58	87	66	78	53	29	11	10	34	18	26	14
Ba	390	425	450	670	340	225	410	480	264	248	63	41	29	59	48	32	45
Sn	8.4	9	10.3	5.7	31	35	27	29	34	18	38	46	81	29	36	51	49
Pb	31	58	45	26	67	48	49	53	38	56	49	52	48	51	43	32	36
Zn	54	61	76	59	54	60	71	46	65	49	48	78	75	47	60	59	63
Ni	7.2	6	5.4	14	3.1	3.3	4.5	3.2	2.5	3.3	1.8	0.9	1.5	2.3	1.9	1.1	1.6
Co	3.9	4.2	3.4	6.8	1.5	1.1	1.2	0.5	0.6	0.8	1.3	0.8	0.9	0.6	0.5	0.9	0.8
Cr	21	19	16	36	10	7	8	9	12	10	10	5	11	9	4	6	8
Nb		32				84		91					62.6		66		70
Ta		2.9				14.2		12.8					18.5		20		16.5
Zr		284				145		124					235		160		113
Hf		9.2				5.6		5.4					12.4		11		5.1
Y		48				82		67					100		56		48
Be	6	5.1	5.8	4.4	9.2	6.9	8.4	6.5	9.2	10	7.3	11	10.3	11.2	10.4	12.5	8.9
B	23	19	28	15	69	84	90	71	93	88	130	125	170	87	94	110	90
F (wt%)	0.14	0.12	0.19	0.09	0.35	0.52	0.3	0.33	0.54	0.4	0.57	0.6	1.2	0.59	0.4	0.53	0.69
K/Rb	145	131	123	160	108	108	94	103	92	76	37	28	42	33	54	39	43
Ba/Rb	1.3	1.3	1.4	3.2	0.86	0.62	0.95	1	0.6	0.47	0.06	0.03	0.03	0.06	0.06	0.03	0.05
Nb/Ta		11				5.9		7.1					3.4		3.3		4.2
Zr/Hf		30.8				26		23					18.9		14.5		22.2

coarse-grained, densely porphyritic and occasionally exhibit a trachytoid fabric and hypidiomorphic granular texture. The mafic minerals are locally glomerocrystic. In the most typical varieties, 30–40% of the K-feldspar megacrysts are surrounded by oligoclase rims 1–2 mm thick, to create a rapakivi-textured mantle. Major mineral phases are perthitic microcline (40–60%), plagioclase (15–25%), quartz (15–30%), biotite (5–10%) and hornblende (2–7%). Accessory phases include allanite, zircon, apatite, titanite, ilmenite, magnetite, and fluorite. Fayalite and wustite globules with native iron cores are found in some samples not bearing quartz (Jenchuraev and Solomovich, 1979).

The medium-grained hastingsite–biotite granites make up small stocks cutting through rapakivi of the Akshiyrak pluton (Akchiy). They also form some of the small plutons (Maybash) (Fig. 1). Major phases are quartz (23–28%), microcline (43–53%), plagioclase (16–21%), biotite (4–6%) and hastingsite (0.5–3.5%). Accessory phases are zircon, allanite, apatite, fluorite, tourmaline, ilmenite and magnetite. The subalkaline amphibole hastingsite forms the anhedral granules, filling the interstitial places among quartz and feldspar. It also forms rims around magnetite.

The fine-grained hastingsite–biotite leucogranites make up numerous dikes cutting through granites of the first and the second intrusive phases. They also form some of the small independent stocks (Jetykait, Aiyransu, and Ara). The rocks are porphyries and consist of quartz (30–32%), microcline (43–53%), plagioclase (22–25%), biotite (3–3.5%) and hastingsite (0.5–1%). Accessory minerals are allanite, apatite, and fluorite. The microgranophyric texture of the mesostasis is indicative of their compositional proximity to the granite eutectic.

The chemical composition of the Jangart complex rapakivi (Table 1) is close to that of the classical rapakivi of the Fennoscandian Shield (Solomovich and Trifonov, 1990). In comparison with the calc–alkali syncollisional granites, having the same SiO_2 content, they are notable for the high alkalinity ($K_2O + N_2O$ ranges from 8.0 to 9.1 wt%) with $K_2O > Na_2O$ and slightly lower contents of CaO, MgO, Al_2O_3. The rocks are metaluminous ($Al_2O_3/(CaO + K_2O + Na_2O) < 1$). The presence of fayalite, wustite, native iron along with high $FeO^t/(FeO^t + MgO)$ ratio are indicative of the low H_2O and O_2 fugacities in the magma, typical of rapakivi granites (Shinkarev and Ivanikov, 1983; Frost et al., 1999).

The trace element contents (Table 1) also correspond to those of the classical rapakivi. The high concentrations of both compatible (Co, Cr, Ni) and incompatible (Rb, Ba, Sn, REE) elements are typical. The fluorine content (0.20–0.35 wt%) is especially high and close to that of rare-metal granite according to Koval (1998).

In comparison with rapakivi granites, the hastingsite–biotite granites are more differentiated. They are richer in SiO_2, Li, Rb, F, B and relatively poor in Al_2O_3, CaO, MgO, FeO^t, Sr, Ba, Co, Ni and Cr. The K/Rb and Ba/Rb ratios are lower accordingly. Such a distribution of elements, as is generally known, is typical of the consecutive intrusive phases in homodromous granitic series. Hastingsite–biotite leucogranites of the third phase are the richest in SiO_2 and the poorest in Al_2O_3, CaO, MgO, FeO^t, Co, Ni and Cr. Li and Rb contents are similar to medium-grained hastingsite–biotite granites, and F is lower (Table 1). The lower La/Yb ratios and Eu anomaly is more pronounced in medium- and fine-grained granites (Table 2, Fig. 3(a)) consistent with fractionation of plagioclase and mafic minerals. The chemical features of the Jangart intrusive complex are similar to metaluminous A-type granites (Frost et al., 1999).

4.2. Inylchek complex

Intrusive rocks of the Inylchek complex stretch along the northwestern portion of the Variscan Collisional belt near the boundary with the Kazakh microcontinent. They are intruded into the Inylchek thrust package (Fig. 1). The complex is composed of small stocks: Tashkoro (8 km^2), Maidadir (6 km^2), Suchodol (4 km^2), Inylchek (2 km^2), Atjailau (1 km^2), and a larger one, Komsomol (20 km^2). The Inylchek complex was also formed by the consecutive emplacement of three intrusive phases (Baybulatov et al., 1983): (1) quartz monzonites; (2) coarse-grained porphyritic biotite granites; (3) medium-grained biotite leucogranites and Li–mica leucogranites.

The quartz monzonites make up an intrusive body (3 km^2) on the northern flank of the Komsomol stock, as well as small xenoliths in other plutons. Major minerals are plagioclase—47.2%, quartz—22%, perthitic microcline—19.5%, biotite—10.3%, pyroxene and amphibole—1.5%. Accessory minerals are apatite, zircon, allanite, titanite, ilmenite, tourmaline and fluorite.

The coarse-grained porphyritic biotite granites dominate the Tashkoro and Maidadir stocks. Major minerals are perthitic microcline (48–50%), plagioclase (15–18%), quartz (23–29%), biotite (5–9%). Accessory phases are zircon, apatite, ilmenite, titanite, rutile, allanite, monazite, thorite, cassiterite, tourmaline and fluorite.

Medium-grained biotite leucogranites cut through the coarse-grained porphyritic biotite granites in stocks of the Tashkoro and Maidadir. They dominate the Inylchek and Atjailau stocks. Towards the apical parts of intrusives, biotite leucogranites grade into Li–mica leucogranites, which are abundant at the current level of erosion. The Li–mica leucogranites make up almost all of the stock of Suhodol and most of the large Komsomol intrusive. The Li–mica leucogranite is a white or greenish rock (the greenish color is caused by the amazonite) with an equigranular, hypidiomorphic granular texture. Quartz is usually rounded and glomerocrystic. Miarolitic fabric is typical. The large cavities are sometimes filled with Li–mica, rare metal pegmatite, containing polychromatic tourmaline. Li–mica granite consists of quartz (33–37%), perthitic microcline (35–38%), albite (25–27%) and Li–mica (4–5%). The Li–mica is zinnwaldite or protolithionite (Baybulatov et

Table 2
Rare-earth element concentration (ppm) of granitic rocks from South Tien Shan

Complex	Jangart				Inylchek					
Pluton	Jangart	Akshiyrak	Maybash	Iransu	Tashkoro		Suchodol			Komsomol
Sample	TF251	TF91	SH500	SH302	T76/3	T67	T99/8	T96/7	T90/1	K1000
Description	Grsy-rpk	Gr-rpk	Has-gr	Has-lcgr	Bi-gr	Bi-gr	Bi-lcgr	Li-lcgr	Li-lcgr	Li-lcgr
La	120	115	86	41	54	72	18	18	18	70
Ce	230	230	170	89	78	96	32	35	38	150
Pr	22	21	16	11	9	12	5.4	7	4.5	20
Nd	100	69	56	37	21	39	14	17.5	14	90
Sm	15	11	13	9	8.8	11	8	8.6	6.7	24
Eu	2	1.6	1	0.6	0.57	1.1	0.19	0.08	0.07	1.2
Gd	16	12	9.1	7.5	6.8	9.6	6.6	8.6	8.2	35
Du	11	7.4	9.3	11.5	4.9	7.2	8.6	8.4	8.9	44
Ho	2.1	1.6	1.8	2.4	1.1	1.8	1.8	2	2	11
Er	4.6	4.9	4.8	5	2.8	3.6	6.8	7.8	8.2	30
Yb	4.7	5	6.4	7.8	2.6	4.1	9.4	6.3	6.9	24
Lu	0.8	0.6	0.65	0.84	0.6	0.78	1.3	1.4	1.2	4.2
La/Yb	25.5	23	13.43	5.4	20.8	17.6	1.9	2.9	2.6	2.9
Eu/Eu	0.39	0.42	0.25	0.21	0.22	0.32	0.08	0.03	0.03	0.12

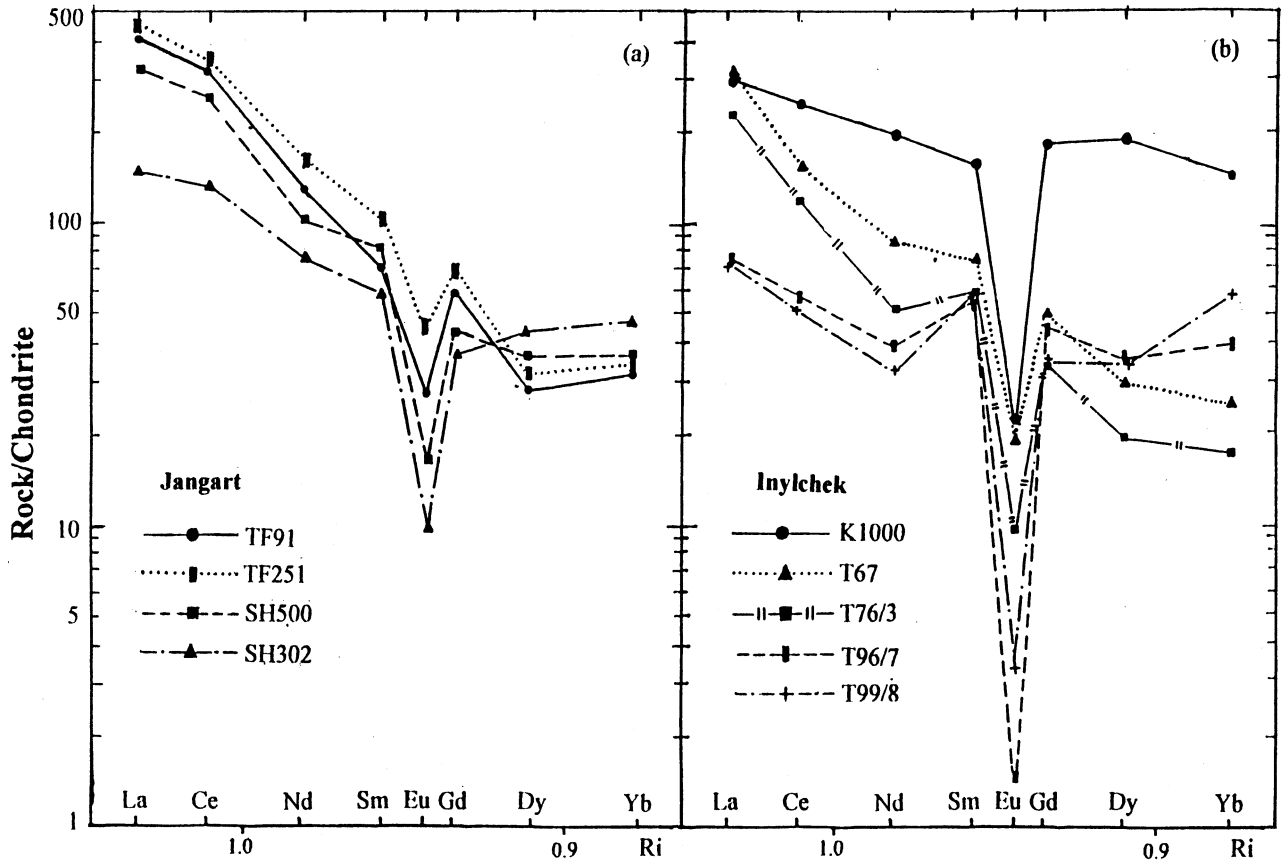

Fig. 3. Chondrite-normalised (Anders and Grevesse, 1989) REE distribution patterns for postcollisional granites from South Tien Shan. R_i is ion radius of element (Å).

Table 3
Rb–Sr isotopic data for granitic rocks from South Tien Shan

Complex	Pluton	Sample	Description	Rb (ppm)	Sr (ppm)	$^{87}Rb/^{86}Sr$	$^{87}Sr/^{86}Sr$	Isochron age (T)	Composite isochron age (T) for the complex
Jangart	Akshiyrak	O291	Granite rapakivi	241.1	119.5	5.768	0.73031	$T = 271 \pm 30$ Ma	$T = 269 \pm 21$ Ma
		O331	Granite rapakivi	175.7	74.54	6.722	0.73239	$Sr_0 = 0.7068 \pm 0.0048$	$Sr_0 = 0.70753 \pm 0.0043$
		O330	Granite-porphyry	196.1	35.66	15.73	0.76335	MSWD = 38	MSWD = 79.1
		O327	Microgranite	267	25.45	30.19	0.82648		
		O334	Aplite	815	4.179	704.7	3.4658		
	Maybash	O302	Hast-granite	317.5	50.06	18.17	0.77056	$T = 264 \pm 8.4$ Ma	
		O306	Hast-granite	318.6	11.15	83.72	1.01697	$Sr_0 = 0.7023 \pm 0.0053$	
	Jeticait	SH500/34	Hast-leucogranite	282	62.43	12.92	0.75799	$T = 269 \pm 43$ Ma	
		O102	Aplite	246.5	40	17.66	0.78453	$Sr_0 = 0.7114 \pm 0.1134$	
		O84	Microgranite	453	20.5	64.32	0.94089	MSWD = 173	
Inylchek	Tashkoro	O435	Bi-granite	371.9	97.33	10.92	0.75354		$T = 269 \pm 8$ Ma
		O436	Microgranite	348.2	84.18	11.83	0.75622		$Sr_0 = 0.70985 \pm 0.00229$
		O108	Granite-porphyry	2233	23.82	296.6	1.84625		MSWD = 14.6
	Suchodol	O010011	Li–mica leucogranite	1022	19.25	160.2	1.32641		
		O182	Granite-porphyry	831.3	18.03	137.8	1.2171		
	Maidadir	O386	Bi-granite	136.9	85.19	4.595	0.75805		
		O413	Bi-granite	318.4	11.87	78.58	1.01134		
	Atjailau	SH39	Bi-granite	411.5	20.84	57.4	0.93175		
		O0999	Granite-porphyry	494.8	166.8	8.465	0.74203		
	Komsomol	SH504/1	Li–mica leucogranite	1002	12.28	254.6	1.69115		
Uchkoshkon	Uchkoshkon[a]	206801	Bi-leucogranite	347.7	94.3	10.72	0.75004	$T = 275 \pm 11$ Ma	
			K-feldspar	516.2	103.3	14.53	0.76454	$Sr_0 = 0.7080 \pm 0.0022$	
		207001	Bi-leucogranite	460.6	76.8	17.45	0.77676	MSWD = 0.7	
		YKS	Bi-leucogranite	398.1	65.6	17.7	0.77707		
		205401	Bi-leucogranite	456.4	41.6	32.13	0.8363	$T = 273 \pm 34$ Ma	
			K-feldspar	756.4	58.11	38.22	0.85994	$Sr_0 = 0.7116 \pm 0.0167$	
		205501	Bi-leucogranite	461.7	14.83	93.38	1.08852	$T = 273 \pm 9$ Ma	
		206601	Bi-leucogranite	571.5	37.76	44.62	0.89899	$Sr_0 = 0.7256 \pm 0.0070$	

[a] Analyzed and reported in Byske et al. (1996). Sr and Rb concentrations determined by isotope dilution. Sr_0 is the initial $^{87}Sr/^{86}Sr$ ratio; MSWD is the mean square of weighted deviates. Isochron ages, Sr_0 and MSWD calculated using the program by Ludwig (1991).

al., 1983). Accessory minerals are zircon, cyrtolite, thorite, monazite, xenotime, cassiterite, columbite, garnet, topaz, fluorite and tourmaline.

All magmatic rocks of the Inylchek complex are peraluminous ($Al_2O_3/(CaO + Na_2O + K_2O) > 1$), rich in K and lithophile trace elements such as Li, Rb, Cs, Be, Sn, B, F (Table 1), the concentrations of which increase in successive intrusive phases and reach a maximum in Li–mica leucogranites. According to the geochemical classification of granites by Tauson (1977), the second phase biotite granites and the third phase biotite leucogranites belong to the geochemical type of rare-metal plumasitic granites (RGP), while Li–mica leucogranites correspond to the Li–F geochemical facies of RGP. The Li–mica leucogranites (Tables 1 and 2) are extremely rich in Li, Rb, Cs, Y, Sn, Be, Nb, Ta, Zn, F, B and heavy rare earth elements (HREE) and very poor in Sr, Ba, Co, Ni, Cr. The low values of K/Rb, Ba/Rb, Nb/Ta, Zr/Hf and La/Yb ratios, as well as an extremely negative Eu anomaly (Fig. 3(b)), are distinctive features of those rocks. The above chemical characteristics of the Inylchek complex granites are similar to aluminous A-type granites according to Forster et al. (1995).

4.3. Uchkoshkon complex

The Uchkoshkon complex intrusives occur in the central portion of the Collisional belt, and intrude the Kokshal overthrust sheet package (Fig. 1) The complex includes the large Uchkoshkon pluton (300 km^2) and relatively small stocks of Pikertyk, Aktash and Sarybulak. The complex consists of two intrusive phases: (1) quartz monzonites, which constitute only 3% of the total exposed area; (2) (main phase) coarse and medium-grained biotite leucogranites.

The quartz monzonites make up most of the Aktash stock and occur as xenoliths in the Uchkoshkon pluton. Essential minerals are plagioclase (—48%), microcline (—25%), quartz (—17%), amphibole (—2%), and biotite (—8%). Accessory minerals are titanite, magnetite, ilmenite, apatite, allanite, and zircon.

The coarse and medium-grained leucogranites of the main phase consist of quartz (28–36%), perthitic microcline (40–46%), plagioclase (16–20%),and biotite (3–6%). Accessory minerals are zircon, cyrtolite, apatite, ilmenite, monazite, xenotime, cassiterite, fluorite, and tourmaline. The wustite globules with the native iron cores are also found in some samples (Jenchuraev and Solomovich, 1979). In places (Pikertyk stock), tourmaline becomes a rock-forming mineral.

In terms of chemical composition (Table 1), leucogranites are intermediate between peraluminous and metaluminous rocks and also rich in K. High concentrations of Li, Rb, Be, Sn, Nb, Ta, B and F bring them close to the geochemical type of RGP. However, Li–F granites are not present in the Uchkoshkon complex.

5. Rb–Sr age of the postcollisional granites

The granite complexes of Jangart, Inylchek and Uchkoshkon must post-date the age of the Silurian to the Upper Carboniferous sedimentary rocks that they intrude. However, their younger age limit is unknown. Previous K–Ar data suggest ages of Middle Carboniferous to the Upper Permian (Catalogue of Radiometry Age Determinations of Rocks of the USSR, 1972). The Rb–Sr data presented here narrow this time interval and constrain the age of the granites.

The Sr isotopic composition of the Jangart complex has been determined on the basis of ten samples (Table 3) representing all intrusive phases as well as the dike series. The samples were collected from the Akshiyrak, Maybash and Jetykait intrusive bodies. All data give an isochron age of 269 ± 21 Ma (Fig. 4(a)) with the mean square of weighted deviation MSWD of 79.1 and an initial $^{87}Sr/^{86}Sr$ ratio $Sr_0 = 0.7075 \pm 0.0043$. The calculations of the Rb–Sr ages and the initial $^{87}Sr/^{86}Sr$ ratios for each intrusive individually (Table 3) show that the plutons are all the same age within error, as are the initial $^{87}Sr/^{86}Sr$ ratios.

The Sr isotopic composition of the Inylchek complex is also represented by ten samples, which were obtained from the intrusive bodies of Tashkoro, Maidadir, Suchodol, Atjailau and Komsomol (Table 3). All isotopic data yield an isochron (Fig. 4(b)) that corresponds to an age of 269 ± 8 Ma (MSWD = 14.6) and $Sr_0 = 0.7099 \pm 0.0023$.

The Rb–Sr isotopic results of the Uchkoshkon complex, listed in Table 3, come only from samples of the largest Uchkoshkon pluton and yield three parallel isochron lines (Fig. 4(c)). The ages of these three groups of samples are identical within error but the initial $^{87}Sr/^{86}Sr$ ratios of the first group ($Sr_0 = 0.7080 \pm 0.0022$) and third group ($Sr_0 = 0.7256 \pm 0.0070$) are distinct. Since all samples were taken from unaltered leucogranites of the main intrusive phase, the variations of the initial $^{87}Sr/^{86}Sr$ ratio are likely caused by heterogeneity of the magma source.

The Sr isotopic dating suggests that the Jangart, Inylchek and Uchkoshkon granites were emplaced synchronously (within error of the age determinations) during the Permian period.

6. Discussion and conclusions

The data presented above describes three coeval granitic complexes emplaced into different thrust sheets in the Saryjaz segment of the South Tien Shan Variscan Collisional Belt. The granite bodies are discordant with the Paleozoic country rocks and their chemical compositions corresponds to those of ‘within plate granites’ by Pearce et al. (1984) (Fig. 2). The granites are considerably younger (Permian) than the main Collisional event, which occurred during Middle and Upper Carboniferous time, and thus are considered postcollisional.

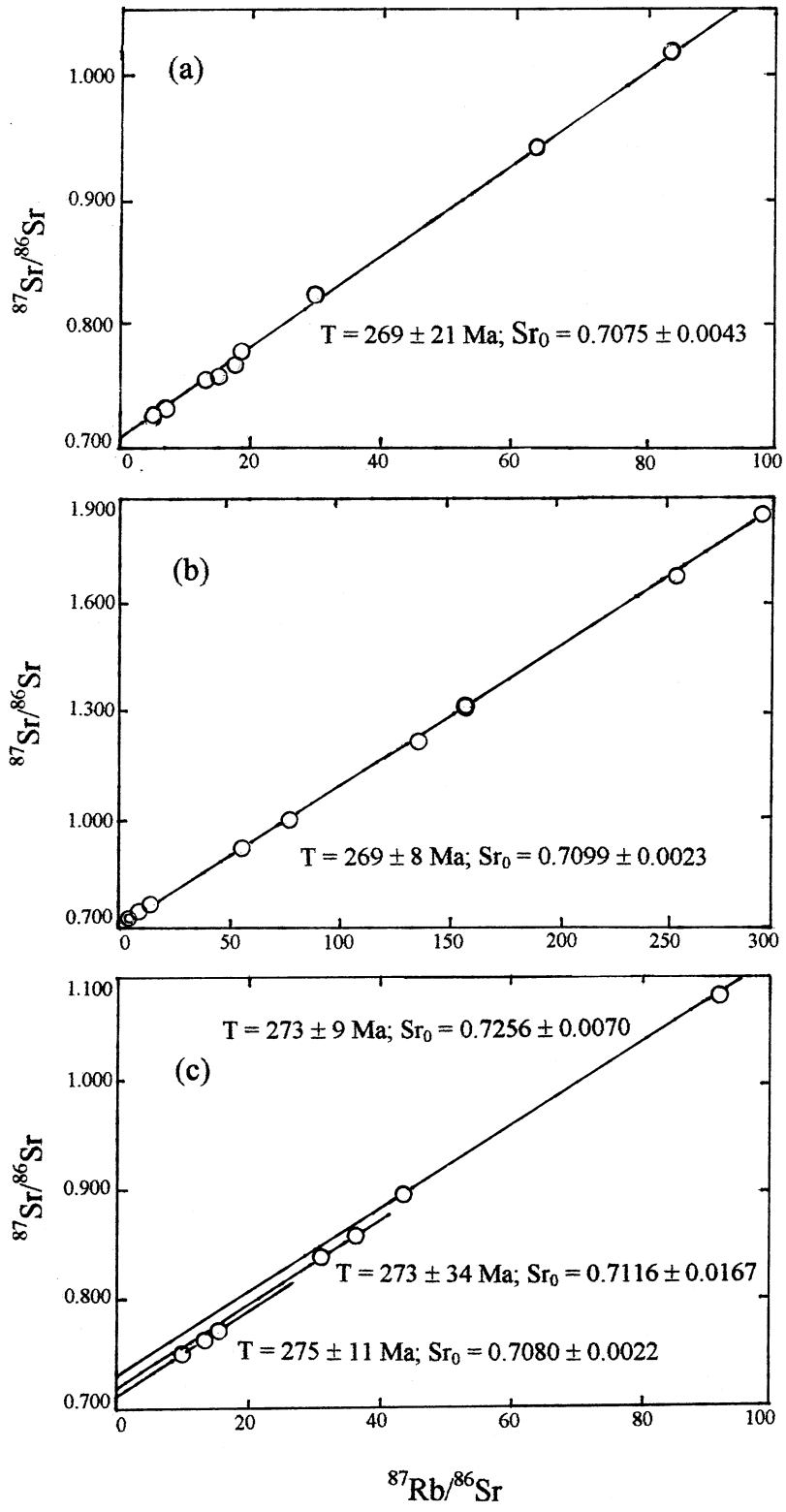

Fig. 4. Rb–Sr isochron diagrams for postcollisional granite complexes of: Jangart (a), Inylchek (b) and Uchkoshkon (c) in South Tien Shan. Regressions calculated using the ISOPLOT program of Ludwig (1991).

Rapakivi, which the Jangart complex rocks resemble, is a texture common in A-type granites (Frost et al., 1999). Many A-type granites are of Precambrian (Proterozoic) age and are widely distributed within the crystalline shields (Shinkarev and Ivanikov, 1983; Anderson, 1983). However, Phanerozoic examples are also known. They include Paleozoic granites of southeastern Australia (Collins et al., 1982) and of Corsica (Poitrasson et al., 1995) and the Mesozoic Younger granites of Nigeria (Jacobsen et al., 1958), Pamir (Levkovskiy, 1975), and the White Mountain Magma Series (Foland and Allen, 1991).

The initial $^{87}Sr/^{86}Sr$ ratio value ($Sr_0 = 0.7075$), obtained for the Jangart rapakivi, is within the range of data from the well-known rapakivi provinces of the Fennoscandian Shield (Shinkarev and Ivanikov, 1983) and southwestern USA (Frost et al., 1999), most of which is within the intervals ($Sr_0 = 0.702–0.706$) and ($Sr_0 = 0.703–0.710$), respectively. The moderately low initial $^{87}Sr/^{86}Sr$ ratio, along with low oxygen and water fugacity, suggest that a radiogenic felsic crustal source is unlikely for A-type granite (Frost and Frost, 1997). However, we have to admit that the problem of rapakivi granites source does not yet have a single solution. Recent petrogenetic models based on experimental results take into consideration isotopic, geochemical and mineralogical compositions, as well as high magma liquidus temperatures and low H_2O and O_2 fugacities. These models indicate a ferrodioritic lower crustal source (Duchesne and Demaiffe, 1987; Scoates et al., 1996; Frost and Frost, 1997). On the other hand, the well-known spatial association of rapakivi granites with ancient platform basement exposures and similarity of their chemical composition to charnockites, enable some geologists to presume a granulite facies felsic lower crust source. According to that point of view, rapakivi is considered a hypobyssal facies of charnockite (Collins et al., 1982; Shinkarev and Ivanikov, 1983). In this connection, the exposure of large masses of the Tarim platform basement within the Paleozoic sedimentary rocks of the Jangart overthrust sheet package (Fig. 1) is of great significance. Moreover, those masses contain small relicts of charnockites and enderbites that were preserved during retrograde metamorphism (Solomovich, 1989). The deeply metamorphosed dehydrated basement of the Precambrian Tarim platform may therefore be considered the most likely source of the Jangart complex granites.

The Inylchek complex represents another type of postcollisional granite. The higher initial $^{87}Sr/^{86}Sr$ ratio ($Sr_0 = 0.7099$), aluminum oversaturation and high concentrations of the incompatible lithophile elements suggest a felsic crustal source for the parental magma. The high Li and Cs (especially Cs) contents in granites rule out derivation of the magma from a source that had experienced a previous episode of melting, otherwise the highly incompatible Cs would have been lost (e.g. London, 1995). The more northern location of the earlier syncollisional calc–alkalic granites in the Atbashy-Inylchek marginal fault zone corroborates this inference. Furthermore, a two-feldspar (microcline and albite) composition of Li–F granites indicates crystallization of these rocks under subsolvus conditions, with H_2O and F fugacities being high. In turn, it indicates that the magma source had not experienced high-grade metamorphism, because H_2O and F would have been also lost. Thus, the newly formed, thickened, relatively weakly metamorphosed South Tien Shan crust could be a likely source of the Inylchek complex granites. The recent detailed isotopic and geochemical study of Li–F granites in the Variscan Erzgebirge, Germany (Forster et al., 1999) has indicated that interlayering of the metagreywackes and quartz–feldspar rocks with the metapelites could be the most appropriate source of Li–F granites. It should be noted that these rocks are common in the Inylchek overthrust sheet package.

The Uchkoshkon complex is characterized by a heterogeneous Sr isotopic composition and the chemical composition of its intrusions differs from Jangart and Inylchek granites. Objective comparison of the three complex granites requires us to take into account two features. First, Li–F granites should be excluded from consideration because extreme F, Li, Rb, Cs, Sn, Be enrichment in those granites was caused partly by high-*T* alteration under the influence of the volatile-rich, highly reactive residual silicate melts and/or aqueous fluids exsolved from them. The quantitative contribution of magmatic and metasomatic processes to the bulk-rock composition is impossible to determine precisely because both can have the same effect for many elements (Forster et al., 1999). Secondly, rocks with the same SiO_2 content should be compared. Taking into account these remarks, the leucogranites of the final intrusive phases are the most suitable for comparison. Together with the similar SiO_2 content, which, probably reflects the same fractionation level, all leucogranites are rich in K along with high $FeO^t/(FeO^t + MgO)$ ratio (Table 1). These peculiarities, as is generally known, are typical for postcollisional leucogranites. At the same time, there are essential distinctions among them.

The Inylchek complex biotite leucogranite are always peraluminous. They exhibit the highest $Al_2O_3/(CaO + Na_2O + K_2O)$ and the lowest $(Na_2O + K_2O)/Al_2O_3$ ratio values. The Inylchek leucogranites are the richest in Li, Rb, Cs, Be, Nb, Ta, Sn, B, F and the poorest in Sr, Ba, Ni, Cr. The lowest K/Rb, Nb/Ta, Zr/Hf, La/Yb ratios are also typical of them (Tables 1 and 2).

In contrast, the Jangart complex biotite and hastingsite leucogranites are always metaluminous. They exhibit the lowest $Al_2O_3/(CaO + K_2O + Na_2O)$ and the highest $(Na_2O + K_2O)/Al_2O_3$ ratios. The Jangart complex leucogranite are the poorest in Li, Rb, Be, Nb, Ta, Sn, B, F and the richest in Sr, Ba, Ni, Cr. The highest K/Rb, Nb/Ta, Zr/Hf, La/Yb ratios are typical of them.

The Uchkoshkon complex biotite leucogranites include both peraluminous and metaluminous rocks. They are also characterized by intermediate contents of most of above mentioned trace elements and their ratios (Table 1). An

intermediate tectonic position of the Uchkoshkon complex granites and their intermediate chemical composition, along with above mentioned Sr-isotopic heterogeneity, suggest a compound magma source, that probably consisted of a mixed melt derived from two heterogeneous sources: the deeply metamorphosed, ancient basement of the Tarim platform and newly formed relatively weakly metamorphosed South Tien Shan crust. These sources could be juxtaposed due to thrusting during the collision and subsequent continental subduction of the Tarim block under the Kazakh microcontinent. Furthermore, it can be inferred that underthrusting of the Tarim block did not exceed the width of the South Tien Shan Collisional Belt, since the complete gradual transition from metaluminous to peraluminous types of postcollisional granites can be observed in the interval between the Kipchak and Atbashy-Inylchek marginal faults.

We conclude that the correlation between granite petrology and geochemistry and geographic location is best explained by changes in crustal composition across the South Tien Shan Variscan Collisional Belt. In the south, the Jangart granites traversed deeply metamorphosed Tarim basement, which yielded little partial melt to the A-type granites. In the northern portion of the belt, the Inylchek leucogranites were formed by partial melting of the greywacke and pelitic rocks of the Collisional belt. Finally, the Uchkoshkon granites, which occupy an intermediate geographic position, were formed from both source rocks, giving them intermediate geochemical characteristics.

Acknowledgements

We would like to thank Dr P.V. Koval and Prof. A.B. Bakirov for helpful discussions. The authors are particularly indebted to Prof. B.A. Natal'in and Prof. C. Frost for detailed reviews and constructive suggestions.

References

Allen, M.B., Sengor, A.M.C., Natal'in, B.A., 1995. Junggar, Turfan and Alakol basins as Late Permian to? Early Triassic extensional structures in a sinistral shear zone in the Altaid orogenic collage, Central Asia. Journal of the Geological Society, London 152, 327–338.

Anders, E., Grevesse, N., 1989. Abundances of the elements: meteoric and solar. Geochimica et Cosmochimica Acta 53, 197–214.

Anderson, J.L., 1983. Proterozoic anorogenic granite plutonism of North America. Geological Society of America, Memoir 161, 133–154.

Baybulatov, E.B., Bokonbayev, K.D., Sabelnikov, S.Ye., Solomovich, L.I., 1983. Granitoidy Vostochnoy Chasti Tyan-Shanya (Granitoids of the Eastern Tien Shan). Ilim Press, Bishkek 242pp. (in Russian).

Bakirov, A.B., Ges, M.D., Khristov, Ye.V., 1989. Domesozoiskaya Paleogeodinamika Tyan-Shana (Premesozoic Geodynamics of the Tien Shan). The Tectonic, Geodynamics and Metallogeny of the Ural—Tien Shan Folding System. Sverdlovsk University Press pp. 10–15 (in Russian).

Bazhenov, M.L., Burtman, V.S., Dvorova, A.V., 1999. Permian paleomagnetism of the Tien Shan fold belt, Central Asia: postcollisional rotations and deformation. Tectonophysics 312, 303–329.

Byske, U.S., 1996. Paleozoiskaya Struktura I Istoriya Ujnogo Tyan-Shanya (Paleozoic Structure and History of the South Tien Shan). St. Petersburg University Press 192pp. (in Russian).

Byske, U.S., Zubkov, S.Ye., Porshniyakov, G.S., 1985. Gertsinidy Atbashy-Kokshaalskogo Raiona Tyan-Shanya (Hercynides of the Atbashy-Kokshaal Region, Tien Shan). Leningrad University Press 190pp. (in Russian).

Byske, U.S., Konopelko, D.L., Shergina, U.P., Kuznetzov, L.V., Rublev, A.G., 1996. Age and formation environment of the Kok-Shaal segment granites, South Tien Shan. St. Petersburg University Bulletin 28, 58–71 (in Russian with English abstract).

Katalog Opredeleniy Vozrasta Gornykh Porod SSSR Radiologicheskimi Metodami, Srednyaya Asiya (Catalogue of Radiometry Age Determinations of Rocks of the USSR: Central Asia). 1972. VSEGEI Press, Leningrad 229pp. (in Russian).

Chen, C., Lu, H., Jia, D., Cai, D., Wu, S., 1997. Closing history of the southern Tianshan oceanic basin, western China: an oblique Collisional orogeny. Tectonophysics 302, 23–40.

Collins, W.J., Beams, S.D., White, A.J.R., Chappell, B.W., 1982. Nature and origin of A-type granites with particular reference to southeastern Australia. Contributions to Mineralogy and Petrology 80, 189–200.

Duchesne, G.C., Demaiffe, D., 1987. Trace elements and anorthosite genesis. Earth and Planetary Science Letters 38, 249–272.

Foland, K.A., Allen, J.C., 1991. Magma sources for Mesozoic anorogenic granites of the White Mountain series, New England, USA. Contribution to Mineralogy and Petrology 109, 195–211.

Forster, H.J., Seltmann, R., Tischendorf, G., 1995. High-fluorine, low-phosphorous A-type (post-collision) silicic magmatism in the Erzgebirge. Extended Abstracts of the Second Symposium on Permocarboniferous Igneous Rocks, Potsdam, 27–29 October. Terra Nostra 7, pp. 32–35.

Forster, H.J., Tischendorf, G., Trumbull, R.B., Gottesmann, B., 1999. Late-collision granites in the Variscan Erzgebirge, Germany. Journal of Petrology 40, 1613–1645.

Frost, C.D., Frost, B.R., 1997. Reduced rapakivi-type granites: the tholeiite connection. Geology 25, 647–650.

Frost, C.D., Frost, B.R., Chamberlain, K.R., Edwards, B.K., 1999. Petrogenesis of the 1.43 Ga Sherman Batholith, SE Wyoming, USA: a reduced, rapakivi-type anorogenic granite. Journal of Petrology 12, 1771–1802.

Gao, J., Li, M., Xiao, X., Tang, Y., He, G., 1997. Paleozoic tectonic evolution of the Tianshan Orogen, northwestern China. Tectonophysics 287, 213–231.

Hamrabaev, I.H., Simon, A.K. (Eds.), 1984. Evolutzia Magmatizma Sredney Azii (The Evolution of Magmatism in Central Asia) Nauka Press, Moscow 276pp. (in Russian).

Jacobsen, R.R.E., Mcleod, W.N., Black, R., 1958. Ring-Complexes in the Younger Granite Province of Northern Nigeria. Geological Society of London Memoir, vol. 1, 72pp.

Jenchuraev, D.D., Solomovich, L.I., 1979. Nahodka Iotcit-Dzelezosoderdzaschih Sharikov V Granitoidakh Kokshal-Tau (The Discovery of the Wustite Globules with Native Iron Cores in Granitoids of the Kokshal Ridge). Zapiski Kirgizskogo Mineralogicheskogo Obschestva (Bulletin of the Kurgyz Mineralogical Society), vol. 8, pp. 51–60 (in Russian).

Khristov, Ye.V., 1989. Kollizionnyye Struktury Saryjazskogo Sintaxsisa (Collisional Structures of the Sayjaz Syntaxis). The Tectonic, Geodynamics and Metallogeny of the Ural—Tien Shan Folding System. Sverdlovsk University Press pp. 154–159 (in Russian).

Knauf, V.I. (Ed.), 1986. Litosfera Tian-Shanya (Lithosphere of the Tien Shan) Nauka Press, Moscow 157pp. (in Russian).

Koval, P.V., 1998. Regionalniy Geochimicheskiy Analis Granitoidov (Regional Geochemical Analysis of Granitoids). Nauka Press, Novosibirsk 492pp. (in Russian).

Levkovskiy, R.Z., 1975. Rapakivi (Rapakivis). Nedra Press, Leningrad 268pp. (in Russian).

London, D., 1995. Geochemical features of peraluminous granites, pegmatites, and rhyolites as source of lithophile metal deposits. In: Thompson,

J.F.H. (Ed.). Magmas, Fluids, and Ore Deposits. Mineralogical Society of Canada Short Course Series, vol. 23, pp. 175–202.

Ludwig, K.R., 1991. ISOPLOT for MS-DOS, a Plotting And Regression Program for Radiogenic Isotope Data, for IBM-PC Compatible Computers, Version 2.75. US Geological Survey Open File Report pp. 91–445.

Pearce, J.A., Harris, N.B.W., Tindle, A.G., 1984. Trace elements discrimination diagrams for the tectonic interpretation of granitic rocks. Journal of Petrology 25, 956–983.

Poitrasson, F., Duthou, J.-L., Pin, C., 1995. The relationship between petrology and Nd isotopes as evidence for contrasting anorogenic granite genesis: example of the Corsican province (SE France). Journal of Petrology 36, 1251–1254.

Porshniyakov, G.S., 1983. Stages of the South Tien Shan folding structure formation. In: Hain, V.E. (Ed.). Tektonika Tian-Shanya I Pamira (Tectonics of the Tien Shan and Pamir). Nauka Press, Moscow, pp. 66–73 (in Russian).

Scoates, J.S., Frost, S.D., Mitchell, J.N., Lindsley, D.H., Frost, B.R., 1996. Residual liquid origin for a monzonitic intrusion in a Mid-Proterozoic anorthosite complex: the Sybille intrusion Laramie anorthosite complex, Wyoming. Geological Society of America Bulletin 108, 1357–1371.

Shinkarev, N.F., Ivanikov, V.V., 1983. Fiziko-khimicheskaya Petrologiya Izverzhennykh Porod (Physicochemical Petrology of Igneous Rocks). Nedra Press, Leningrad 267pp. (in Russian).

Solomovich, L.I., 1989. Rapakivi granites of the South Tien Shan. In: Asanaliev, U.A. (Ed.). Geologicheskiye formatsii I rudonosnost' Kirgizii (The Geological Associations and Mineral Potential of Kyrgyzstan). Frunze Polytechnic Institute Press pp. 146–152 (in Russian).

Solomovich, L.I., Malukova, N.N., 2000. Geokhimicheskiye tipy I potentsial'naya rudonosnost' gertsinskich granitoidov Kyrgyzstana (The geochemical types and mineralisation of the Hercynian granitoids of the Kyrgyzstan). Kyrgyz Mining and Metallurgical Institute Bulletin 1, 51–68 (in Russian).

Solomovich, L.I., Trifonov, B.A., 1990. The association of rapakivi granites, alkaline rocks, and carbonatites in the Tien Shan. Zapiski Vsesoyuznogo Mineralogicheskogo Obshchestva (Bulletin of the Soviet Union Mineralogical Society) 6, 46–59 (in Russian).

Tauson, L.V., 1977. Geochemicheskie Tipy I Potencialnaya Rudonosnost Granitoidov (Geochemical Types and Potential Ore-Bearing of Granitoids). Nauka Press, Moscow 280pp. (in Russian).

Trifonov, B.A., Solomovich, L.I., 1993. Geological structure and ore-magmatic zoning of the Saryjaz tin ore-bearing region. Geologiya Rudnich Mestorozhdeniy (Geology of Ore Deposits) 35, 44–52 (in Russian).

Zonenshine, L.P., Kuzmin, M.I., Natapov, L.M., 1990. Tektonika Litosfernykh Plit Territorii SSSR (Plate Tectonics of the USSR Territory), vol. 2. Nedra Press, Moscow 327pp. (in Russian).